LIGO - T890018-00-R

41a

List of 3/1/89

FILE: error21989.tex

FROM: RW (Feb 19,1989)

TO: Everybody

CONCERNING: An error in the Memo on "Optical Properties of the LIGO beam tubes

An error was made in the equation for the intensity scattering coefficient for the almost smooth surface. The third equation from the bottom of page 6 should read for the case $g << 1$

$$< \rho\rho* >= e^{-g}\left(\rho_0{}^2 + \frac{\pi g T^2 F^2}{A} e^{\frac{-(v_x{}^2+v_y{}^2)T^2}{4}}\right) \qquad g << 1$$

Which now includes g in the diffuse scattered part.

The error propagated in to EQ 1 on page 7 which should read

$$G(\alpha,\beta,\phi) = \left(\frac{2\pi\sigma}{\lambda}\right)^2 \left(\frac{\pi T^2}{\lambda^2}\right) (1 + sin(\alpha)sin(\beta) - cos(\alpha)cos(\beta)cos(\phi))^2 \times$$

$$e^{-\left(\frac{2\pi\sigma}{\lambda}\right)^2 (sin(\alpha)+sin(\beta))^2} e^{-\left(\frac{\pi T}{\lambda}\right)^2 \left(cos^2(\alpha)+cos^2(\beta)-2cos(\alpha)cos(\beta)cos(\phi)\right)} \qquad \text{EQ 1}$$

I never noticed the error since the almost smooth case was not used in any of the calculations associated with the memo, the calculations in the memo should be OK. The almost smooth case has become important now in specifying the smoothness of the baffles to avoid backscattering. These calculations uncovered the mistake.

LIGO-T890018-00-R

#41

List of 3/1/89

FILE: ROUGHSURF.TEX

MEMO: Optical Properties of the LIGO Beam Tubes

TO: Althouse

FROM: RW (January 17, 1989)

OPTICAL PROPERTIES OF THE LIGO BEAM TUBES

The memo deals with the propagation of stray light along the LIGO beam tubes. The number, height, and shape of the baffles depends on the propagation of light by the tubes themselves. Kip has considered many different mechanisms of diffraction and reflection by baffles in the tubes, the most serious mechanism he has uncovered are rays that leave baffles after a small angle diffraction and then continue to propagate at small glancing angles along the tube almost unattenuated. The purpose of the memo is to look a little harder at the exact nature of the problem and to determine a good number for the maximum glancing angle rays that must be converted into larger glancing angle rays by the baffle system. This sets one of the constraints on the baffling.

The memo is in several parts.

1) A calculation of the tube reflectivity for both parallel and perpendicular polarizations.

2) The attenuation of the tube in db per 100 meters of tube length due to reflection losses alone as a function of the angle of incidence (complement of the grazing angle).

3) The attenuation of the coherent propagation due to tube roughness modelled as a surface with a Gaussian distribution of hills and valleys having a variance σ and an exponential isotropic autocorrelation function characterized by the correlation length T.

4) The redistribution of light by this model surface through diffuse scattering and the calculation of an effective reflectivity at grazing incidence due to diffuse scattering.

5) The "attenuation" of glancing rays in db per 100 meters of tube length due to diffuse scattering into larger grazing angles, the scattered light is subsequently attenuated by the imperfect reflectivity of the walls.

References:

1. *The Scattering of Electromagnetic Waves from Rough Surfaces*

Beckmann,P and Spizzichino,A. Pergamon Press 1963

2.*Scattering from Optical Surfaces* Elson,J, Bennett,H.E., Bennett,J.M. in Applied Optics and Optical Engineering Vol VII, p 191 1979, Academic Press

3. *Diffuse Reflection from a Plane Surface* Look,D.C. JOSA, 55,1628, 1965.

4. *Roughness characterization of smooth machined surfaces by light scattering* Stover,J.C. Applied Optics 14,1796,1975.

5. *A Note on Scattering from a Slightly Rough Surface* Swift, C.T. IEEE Transactions on Antennas and Propagation (V?) 561, 1970.

6. *Principles of Optics* Born,M.,Wolf,E. Pergamon Press 1975.

Reflection by metals

The reflection by metals is characterized by both polarization and conduction currents so that the dielectric constant and therefore the index of refraction are complex. The optical constants of iron, an unspecified steel and chromium are given in the AIP Handbook. I have not been able to find the optical properties of 304 Stainless steel but I don't expect it to be very different than the steel listed.

The complex index of refraction is defined as

$$N = n - ik$$

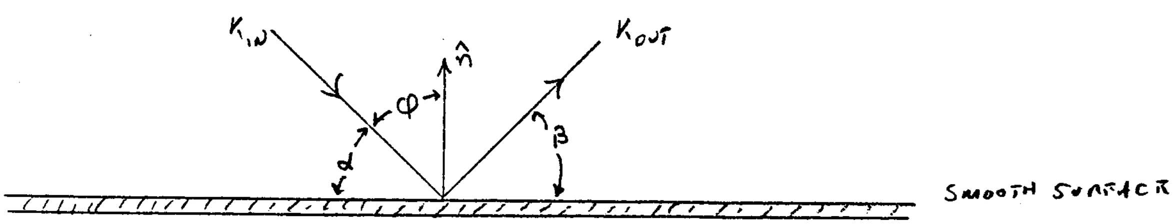

and the reflectivities as a function of angle of incidence are given as

$$R_\perp = \left(\frac{a^2 + b^2 - 2a cos(\phi) + cos^2(\phi)}{a^2 + b^2 + 2a cos(\phi) + cos^2(\phi)}\right)$$

$$R_\parallel = R_\perp \left(\frac{a^2 + b^2 - 2a sin(\phi) tan(\phi) + sin^2(\phi) tan^2(\phi)}{a^2 + b^2 + 2a sin(\phi) tan(\phi) + sin^2(\phi) tan^2(\phi)}\right)$$

$$2a^2 = \left((n^2 - k^2 - sin^2(\phi))^2 + (2nk)^2\right)^{1/2} + \left(n^2 - k^2 - sin^2(\phi)\right)$$

$$2b^2 = \left((n^2 - k^2 - sin^2(\phi))^2 + (2nk)^2\right)^{1/2} - \left(n^2 - k^2 - sin^2(\phi)\right)$$

Typical values are given in the table below

metal	$\lambda(\mu)$	n	k	a	b	$R(\phi = 0)$
chromium	0.58	2.97	4.85	2.925	4.925	.69
iron	0.5	3.022	3.845	2.96	3.926	.61
iron	1.0	3.81	4.44	3.755	4.505	.644
steel	0.5	2.09	3.14	2.019	3.251	.57

Figure 1,2,3 show the reflectivity for iron,chromium and steel, an interesting thing is the imperfect Brewster angle condition at large angles of incidence due to the imaginary part of the index, k, in the parallel component.

A useful approximation near grazing incidence expressed in terms of the grazing angle is

$$R_\perp(\alpha) \approx 1 - \left(\frac{4\alpha a}{a^2 + b^2}\right) = 1 - 9.6 \times 10^{-3} \alpha(degrees) \quad \text{for steel}$$

Attenuation along the tube due to reflection loss

The tubes act like light pipes. The distance between specular (no scattering) hits for a ray at grazing angle, α, is

$$l(\alpha) = \frac{2a}{tan(\alpha)}$$

where a is the tube radius. The transmission along the tube in a length L is given by

$$T(\alpha) \approx R_{\perp}(\alpha)^{Ltan(\alpha)/2a}$$

or the attenuation in db is

$$ATT(db) = 10\,(Ltan(\alpha)/2a)\,log_{10}(R_{\perp})$$

Figures 4,5 show the attenuation of a 4 km long 48 inch diameter tube as a function of the grazing angle, the smallest grazing angle that still makes an encounter with the wall is .0175 degrees. Figures 6,7 show the same attenuation in db per 100 meters of steel tube as a function of grazing angle. Be careful with these curves since the minimum grazing angle that makes one encounter with the wall in 100 meters is .7 degrees, nevertheless this is a useful curve in calculating the attenuation of longer systems and when compared with the effect of diffuse scattering to be considered later in the memo.

The important property the curves show is that once grazing rays at small angles have been converted to rays with angles of 5 degrees and larger the attenuation in the tubes and therefore the net absorption of the stray light becomes enormous. This is the basis for the baffling strategy to reduce stray light. It is the "blackening" mechanism of the tubes and the means for isotropizing the stray light at the exit pupil of the system.

Scattering by the tube walls

The reflection calculations of the previous section assume that the tube surface does not scatter, in other words, a light beam encountering the tube wall hits and leaves the wall at equal grazing angles and is attenuated only by the loss on reflection. If the tube wall is not perfectly smooth (smoothness will be defined below), the light will also scatter into other angles. The scattering is analysed by dividing it into a coherent process and a diffuse or random process. In order to understand this, imagine a light beam hitting the tube wall at grazing angle α and ask how much of the light will be collected by a collimating system directed along the exit glancing angle β around a small solid angle $d\Omega$. The coherent contribution will be that part of the light collected which still retains the phase relations of the original incident wavefront across the collected wavefront. If the original source of the light was a point source, say a single bad patch on one of the mirrors, the coherent scattered wave will still be able to be brought to a diffraction limited point focus. The coherent part of the scattered wave includes the specular reflection at $\alpha = \beta$ and has an angular distribution peaked in this direction. The area of the wall that participates in the coherent part of the scattering is determined by the first Fresnel zone along the tube wall.

The coherent scattering is the most harmful component since fluctuations in phase of the coherent part when driven by wall motions will make phase noise in the interferogram after recombination with the main beams. What is in our favor is the rapid attenuation of the coherent component with increasing surface roughness, these issues will be discussed more adequately below.

The diffuse component does not retain the phase correlations across the wavefront of the incident beam. The diffuse component has a different, generally broader, angular distribution than the coherent component but also tends to peak around the specular direction. The relevant parameters in diffuse scattering are both the surface roughness as well as the correlation length of the roughness which together establish a typical slope distribution for the surface. You see this when looking out of an airplane window at the "reflection" of the sun from the ground, there is usually a bright spot at the specular point even when flying over fields. The specular point is easily visible over water but this scattering may still be dominated by the coherent component depending on the water wave amplitude and wavelength. One way to imagine the diffuse scattering is as the incoherent superposition of many wavelets heading into the direction around β but from different facets of the surface which are separated by more than $\lambda/2$ along rays directed toward β. The angular redistribution of the light by diffuse scattering will be discussed in detail below.

Characterization of the surface and the scattering

Much of this section comes from reference 1 but with extensive corrections since the book has many errors.

The surface, extending locally in the x and y direction, will be characterized by a Gaussian distribution of surface irregularities in the z direction. If the mean surface is at $z = 0$ the distribution of the surface, assumed isotropic in x and y, is given by

$$P(z) = \frac{1}{2\pi\sigma} e^{-z^2/2\sigma^2}$$

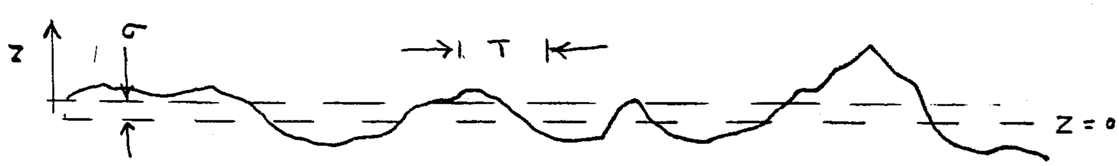

ROUGH SURFACE

$P(z)$ is the probability that the surface has an excursion z at some point x,y; the rms excursion is σ. By assuming that the surface is isotropic, the joint probability distribution of finding a surface excursion difference between two points on the surface becomes only a function of the separation of the points and not a function of the direction in the xy plane

- this may not be a good assumption for surfaces that have been treated by rolling or other forming processes that are anisotropic. The autocorrelation function of the surface is

$$\Phi(\tau) \equiv (1/A) \int_0^{2\pi} \int_0^R z(0)z(\tau)\,d\phi\, r\,dr = \sigma^2 e^{-(\tau/T)^2}$$

A is the averaging area defined by the largest separation R. The specific form of the autocorrelation function (right term in equation) is another assumption about the surface. T is the typical correlation length of an excursion, z, on the surface. The two dimensional probability distribution of finding a surface irregularity z_1 at one place and another irregularity, z_2, at another place a distance τ away is given by

$$P(z_1, z_2) = \frac{1}{2\pi\sigma^2\sqrt{1-C^2}} e^{-\left(\frac{z_1{}^2 - 2Cz_1z_2 + z_2{}^2}{2\sigma^2(1-C^2)}\right)} \quad \text{where} \quad C = \Phi(\tau)/\sigma^2$$

The slope of the surface, ψ, also has a Gaussian distribution,

$$P(\psi) = \left(\frac{T}{2\sigma\sqrt{\pi}cos^2(\psi)}\right) e^{\frac{-T^2 tan^2(\psi)}{4\sigma^2}}$$

The scattering from the surface is calculated from Kirchoff theory, much as in Kip's paper, under the assumption that the second derivative of the surface shape is small enough so that the radius of the best fit sphere to a local region of the surface is still much larger than λ. The scattering amplitude, ρ is defined as the ratio of the actual field in the receiving direction divided by the field that would occur in the same direction if the surface were perfectly smooth and reoriented so that the receiving direction intercepts the specular beam. This definition finesses the diffraction due to finite area of illumination. The scattering amplitude becomes proportional to the two dimensional Fourier transform of the surface irregularities modulated by angular functions that depend on both the incident and exit directions.

SCATTERING GEOMETRY

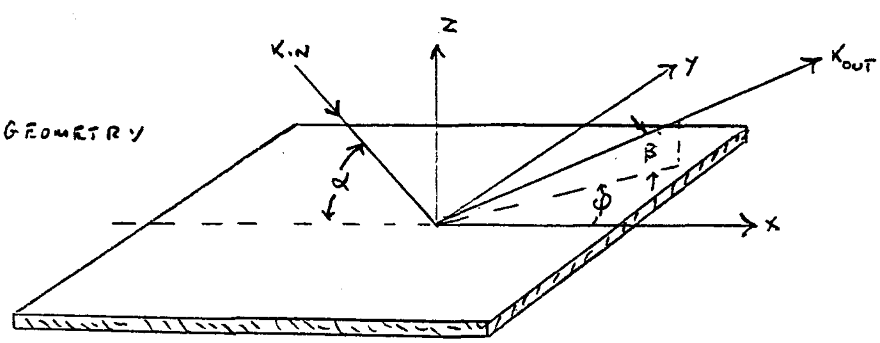

The scattering amplitude, ρ, is

$$\rho = (F(\alpha, \beta, \phi)/A) \int\int_A e^{iV\cdot r} dx dy$$

where

$$F(\alpha,\beta,\phi) = \frac{1 + sin(\alpha)sin(\beta) - cos(\alpha)cos(\beta)cos(\phi)}{sin(\alpha)(sin(\alpha) + sin(\beta))}$$

and

$$V = K_{in} - K_{out} = k\left((cos(\alpha) - cos(\beta)cos(\phi))X - cos(\beta)sin(\phi)Y - (sin(\alpha) + sin(\beta))Z\right)$$

$$V \cdot V = {v_x}^2 + {v_y}^2 + {v_z}^2 \qquad \text{and} \qquad k = \frac{2\pi}{\lambda}$$

To determine the scattering angular distribution, the surface is analysed as a set of random two dimensional diffraction gratings, by taking the Fourier transform of the surface with modulating functions determined by the incident and exit directions. Reference 1 (p 80 - 89, and appendix C) shows how this is done.

The result of the calculation for the intensity scattering coefficient is

$$< \rho\rho* >= e^{-g}\left({\rho_0}^2 + \frac{\pi T^2 F^2}{A}\sum_{m=1}^{\infty}\frac{g^m}{m!m}e^{\frac{-({v_x}^2+{v_y}^2)T^2}{4m}}\right)$$

g is the Rayleigh roughness parameter given by

$$\sqrt{g} = v_z\sigma = \frac{2\pi\sigma}{\lambda}(sin(\alpha) + sin(\beta))$$

The first term in the brackets is the coherent scattering and the second the diffuse scattering. An almost smooth surface is characterized by $g << 1$ while a rough surface by $g >> 1$. A is the area of the surface illuminated. ${\rho_0}^2$ is the coherent intensity scattering coefficient which for a rectangular illuminated area of dimensions l_x and l_y is given by

$${\rho_0}^2 = \left(\frac{sin(v_x l_x)sin(v_y l_y)}{l_x l_y}\right)^2$$

The intensity scattering coefficient for the limiting cases are

$$< \rho\rho* >= e^{-g}\left({\rho_0}^2 + \frac{\pi T^2 F^2}{A}e^{\frac{-({v_x}^2+{v_y}^2)T^2}{4}}\right) \qquad g << 1$$

$$< \rho\rho* >= \left(\frac{\pi F^2 T^2}{A v_z^2 \sigma^2}\right)e^{\frac{-({v_x}^2+{v_y}^2)T^2}{4v_z^2\sigma^2}} \qquad g >> 1$$

A useful quantity for the scattering calculation in the tube is the mean power reflection coefficient for the surface A, this is given by

$$R =< \rho\rho* > \frac{A^2 sin^2(\alpha)}{\lambda^2 r^2}$$

r is the distance between the receiver and the surface patch of area A.

For the diffuse scattering the most useful quantity is the power scattered per solid angle divided by the incident power.

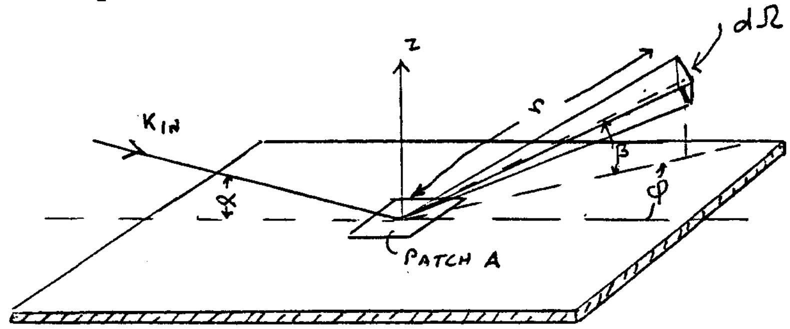

$$G(\alpha,\beta,\phi) = \frac{(dP_{scat}(\beta,\phi)/d\Omega)}{P_{inc}(\alpha)} = Rr^2/A$$

The specific formulations used in the rest of the memo to estimate the diffuse scattering are: for $g << 1$

$$G(\alpha,\beta,\phi) = \left(\frac{\pi T^2}{\lambda^2}\right)\left(\frac{1 + sin(\alpha)sin(\beta) - cos(\alpha)cos(\beta)cos(\phi)}{sin(\alpha) + sin(\beta)}\right)^2 \times$$

$$e^{-\left(\frac{2\pi\sigma}{\lambda}\right)^2 (sin(\alpha)+sin(\beta))^2} e^{-\left(\frac{\pi T}{\lambda}\right)^2 \left(cos^2(\alpha)+cos^2(\beta)-2cos(\alpha)cos(\beta)cos(\phi)\right)} \qquad \text{EQ 1}$$

and for rough surfaces $g >> 1$

$$G(\alpha,\beta,\phi) = \frac{1/4\pi(T/\sigma)^2(1 + sin(\alpha)sin(\beta) - cos(\alpha)cos(\beta)cos(\phi))^2}{(sin(\alpha) + sin(\beta))^4} \times$$

$$e^{-(T/2\sigma)^2 \frac{\left(cos^2(\alpha)+cos^2(\beta)-2cos(\alpha)cos(\beta)cos(\phi)\right)}{(sin(\alpha)+sin(\beta))^2}} \qquad \text{EQ 2}$$

Attenuation of coherent propagation in the tubes

The coherent part of the scattering is the most serious in producing phase noise at the interferometer output. The area along the tube walls that could contribute to the coherent scattering are the Fresnel zones on the tube walls. The Fresnel zone here is the area along the tube wall for which reflections of a plane wave originating at one end of the tube would arrive at the other end with a net phase difference across the wavefront of less than π. The Fresnel zone is an ellipse on the tube wall with the major axis running along the tube and the minor axis along the azimuthal direction. Straight forward geometry but miserable algebra is needed to determine the major and minor axes of the ellipse as a function of distance, z, along the tube of length L and radius a. Define

$$A = (z^2 + a^2)^{1/2} \qquad \text{and} \qquad B = (z^2 + u^2)^{1/2}$$

$$u = L - z$$

$$G = \left(\frac{A^2B^2(uA - zB)}{A^2B^3 - z^2B^3 - u^2A^3 + A^3B^2}\right)$$

$$H = \left(\frac{A^2B^3 - z^2B^3 - u^2A^3 + A^3B^2}{A^3B^3}\right)$$

then the semimajor axis of the ellipse becomes

$$z_1 = G + \left(G^2 + \frac{\lambda}{H}\right)^{1/2}$$

Near the middle of the tube the semimajor axis becomes

$$z_1(L/2) = \frac{(L^3\lambda)^{1/2}}{4a}$$

The minor axis of the ellipse changes little over the tube length and is given by

$$y_1 = (\lambda L)^{1/2}/2$$

Figures 8,9 show the major axis of the Fresnel zone ellipse as a function of fractional distance down the tube. The curve is symmetric about the middle of the tube. The Fresnel zone at the middle of the 4km tube is 73 meters long and becomes smaller as one gets closer to the tube ends. The importance of the zone is that the phase of the beams hitting the Fresnel zones and collected at the exit pupil will vary with the motion of the walls and could cause phase noise in the interferometer output when recombined with the main beam.

The equivalent power reflection coefficient for coherent scattering from EQ 1 is

$$R_{coh} = e^{-(\frac{4\pi\sigma sin(\alpha)}{\lambda})^2}$$

It is worth noting that the total power removed from the coherent part does not depend on the correlation length, T, but only on the Rayleigh roughness in the limit $g << 1$. (This is also true for mirrors at normal incidence. The relations for normal incidence on slightly rough surfaces are important for our mirrors. The formulation for Gaussian surfaces given in the previous section will be applied to the scattering angular distribution measurements that have been made on mirrors in another memo.)

The transmission of the coherently scattered component by multiple reflections from the tube walls is given by

$$T(\alpha) = R_{coh}^{\frac{Ltan(\alpha)}{2a}}$$

expressed as an attenuation in db for a length L

$$ATT(db) = -343(\sigma/\lambda)^2(L/a)sin^2(\alpha)tan(\alpha)$$

Figures 10,11 show the attenuation of coherent propagation in db per 100 meters of tube vs the incident grazing angle for a set of σ/λ. The power removed from the coherent part goes into diffuse scattering which will be considered next.

The redistribution of light by diffuse scattering

The case that has been analysed here is for a rough surface, $g >> 1$. If we intend to roughen tube walls or misalign individual sections of the tube to gain the benefit of the attenuation of the scattering propagation, it only makes sense to look at the rough case. The diffuse scattering is described by EQ 2. The set of figures 12 - 36 show the angular distribution, $G(\alpha, \beta, \phi)$. Each figure is a plot of the diffuse scattering distribution toward β and fixed ϕ for a single value of α. The curves show the distribution for a set of T/σ. (I realize in this age of computer graphics this is a clumsy way to present the 3 dimensional function but so be it.)

The curves show some simple properties.

1) For surfaces with T/σ between 1 and 3 the scattering is almost isotropic for all input angles even grazing angles. One can see the approach to a Lambertian surface. This is no miracle since average surface slopes are large ranging from 45 to 18 degrees. The scattering distribution is most likely underestimated because it does not include shadowing of one part of the surface by another. This should become increasingly important at small brazing angles.

2) For surfaces with long correlation lengths/rms roughness, smaller average slopes, the diffuse scattering peaks in the specular direction with an angular width at the 1/2 power point of $\approx 400\sigma/T$ (degrees). Just what might be expected if light were reflected from a surface with slopes $\pm\sigma/T$.

To determine the attenuation of the diffuse scattering, the integral of EQ 2 was performed numerically over a full 2π solid angle. The integrals for various values of T/σ as a function of α are shown in figure 37. The integrals are miserable requiring double precision and many mesh points (10^7) to stabilize numerically. The salient features of the integral curves are the following.

1) The total power diffusely scattered near grazing incidence varies as σ/T in the rough surface model.

2) The conversion of small grazing angle rays to isotropic ones grows rapidly with increasing grazing angle.

Figures 38 and 39 show the attenuation of rays incident at grazing angle α due both to reflection loss and diffuse scattering loss in db per 100 meters of tube. The approximation being made in these curves is that the power diffusely scattered is indeed lost from the beam so that the equivalent reflectivity is $1 - P_{scat}/P_{inc}$. The approximation neglects the diffusely scattered beam that goes back into the original specular direction. The figures to compare are 6,7 with 38,39 which show the large gain in attenuation at small grazing angles that can be made over just reflection loss by roughening the tube walls.

A table of some cases, summarized from figures and equations

$\lambda = 0.5\mu$

σ/λ	σ (cm)	α (degrees)	g	db_{coh}(4km)	T/σ	T (cm)	$db_{ds \times rf}$ (4km)
100	.005	.0175	.147	.64	1	.005	3.78
1000	.05	.0175	14.7	6.41	1	.05	3.78
1000	.05	.0175	14.7	6.41	3	.15	1.07
10000	.5	.0175	1.47×10^3	6.4×10^3	1	.5	3.78
100	.005	.1	4.81	120	1	.005	21.6
1000	.05	.1	481	1.2×10^4	1	.05	21.6
1000	.05	.1	481	1.2×10^4	3	.15	6
10000	.5	.1	4.81×10^4	1.2×10^6	1	.5	21.6
100	.005	.3	43.3	3.2×10^3	1	.005	65
1000	.05	.3	4.3×10^3	3.2×10^5	1	.05	65
1000	.05	.3	4.3×10^3	3.2×10^5	3	.15	18
100	.005	.5	120	1.5×10^4	1	.005	108
100	.005	1	480	1.2×10^5	1	.005	216

Recommendations and Summary

Roughening the tube walls helps to bring the critical angle to less than 1 degree and possibly as little as .5 degrees. I need further discussions with Kip concerning the relative importance of the coherent and diffuse attenuation, before a recommendation to the project can be made. Another matter that needs immediate attention is the actual roughness of manufactured tubing. I intend to settle these issues on my visit this coming week (Jan 23, 1989).

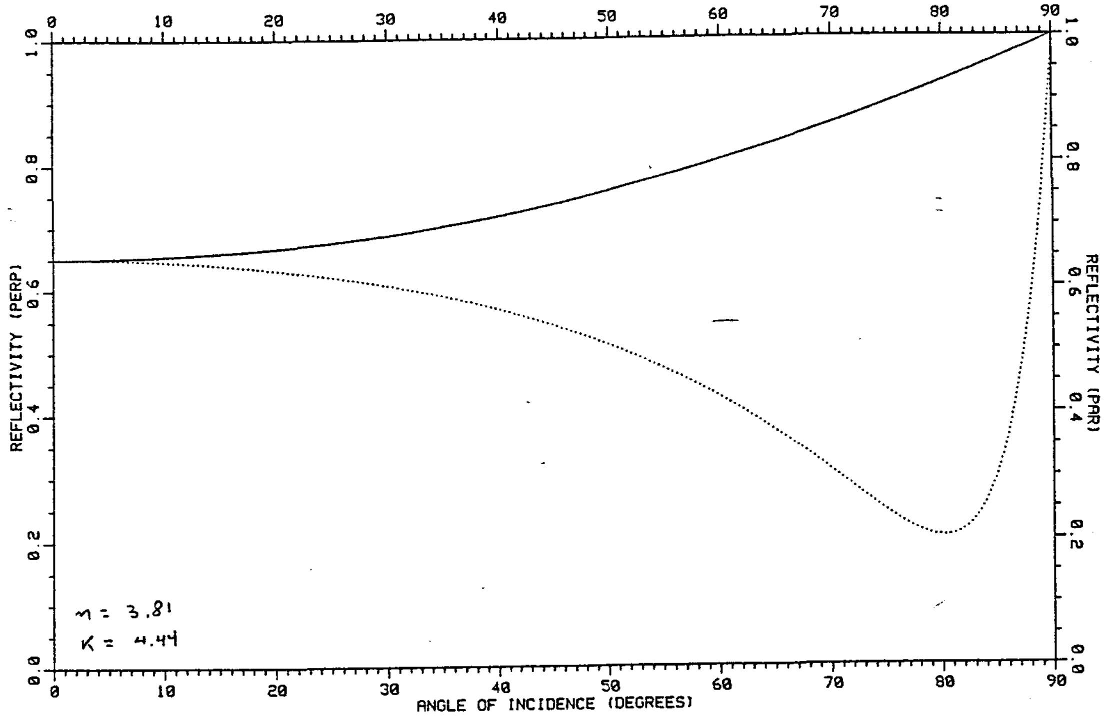

REFLECTIVITY OF IRON AT 1 MICRON

FIGURE 1

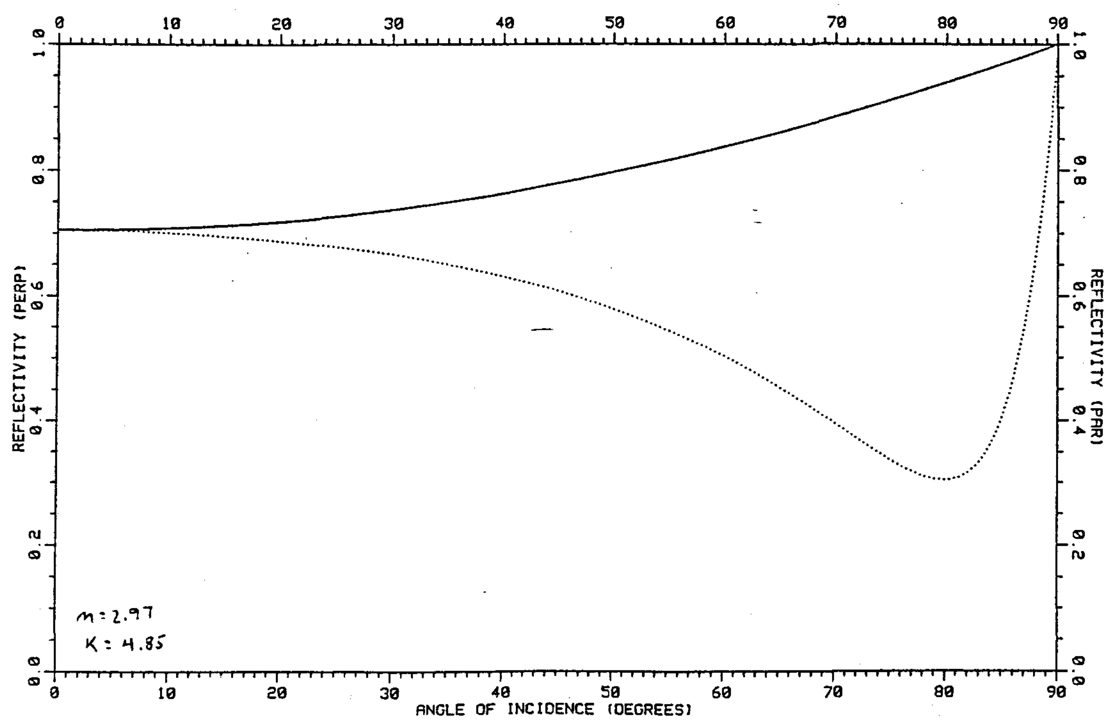

REFLECTIVITY OF CHROMIUM AT .58 MICRONS

FIGURE 2

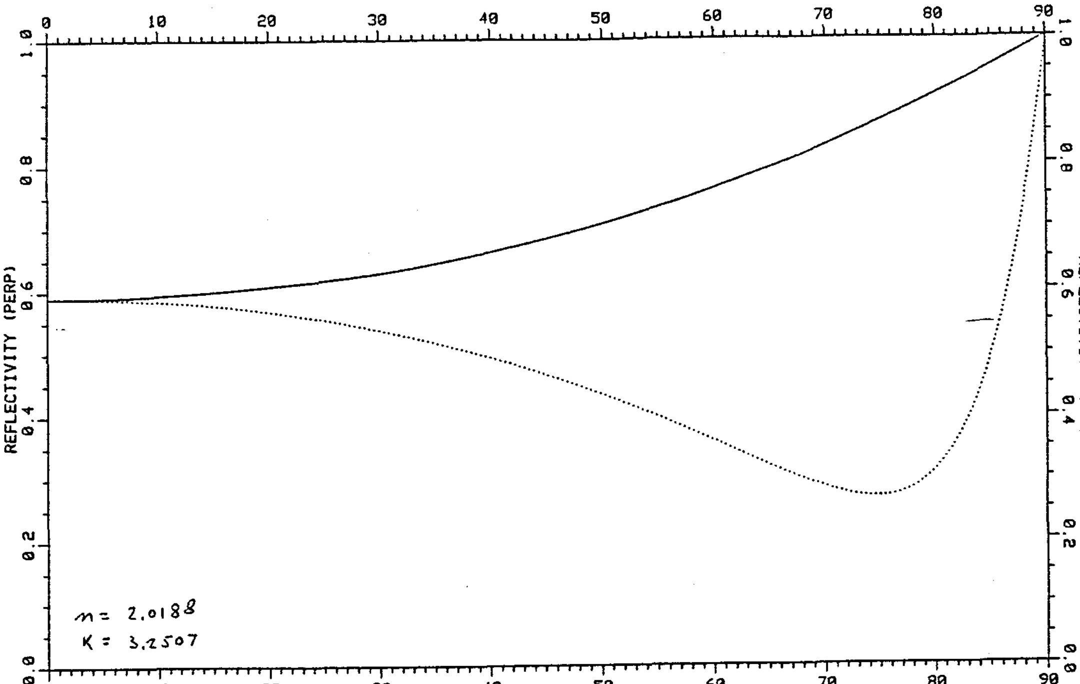

REFLECTIVITY OF STEEL AT 0.5 MICRONS

Figure 3

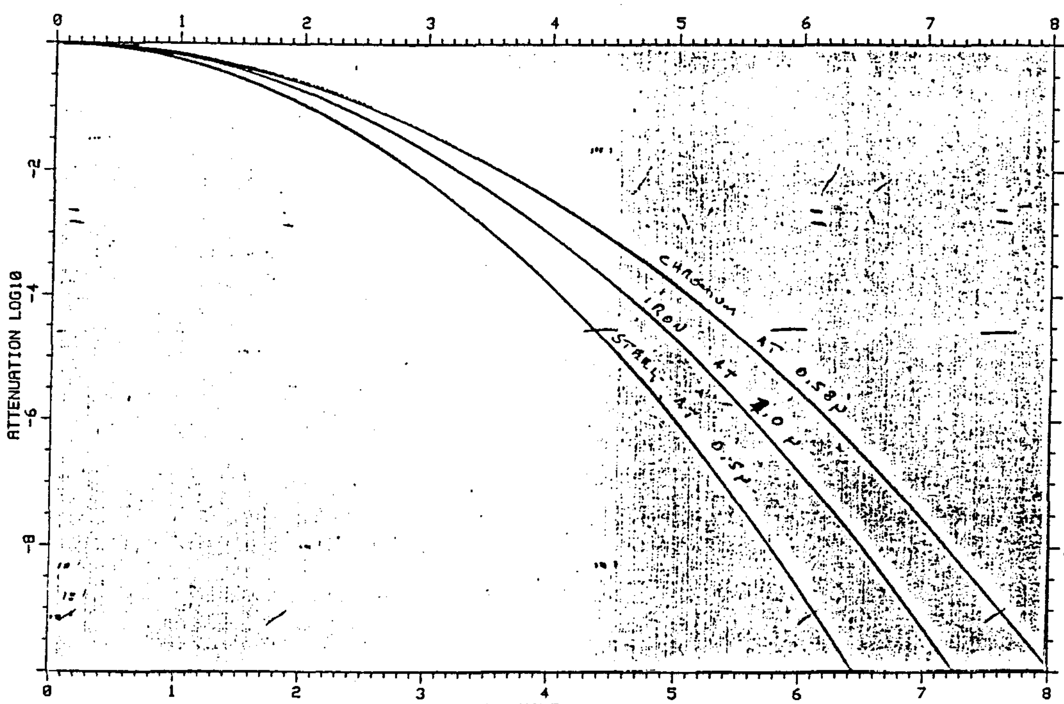

Attenuation 4Km long 48" diameter tube

Figure 4

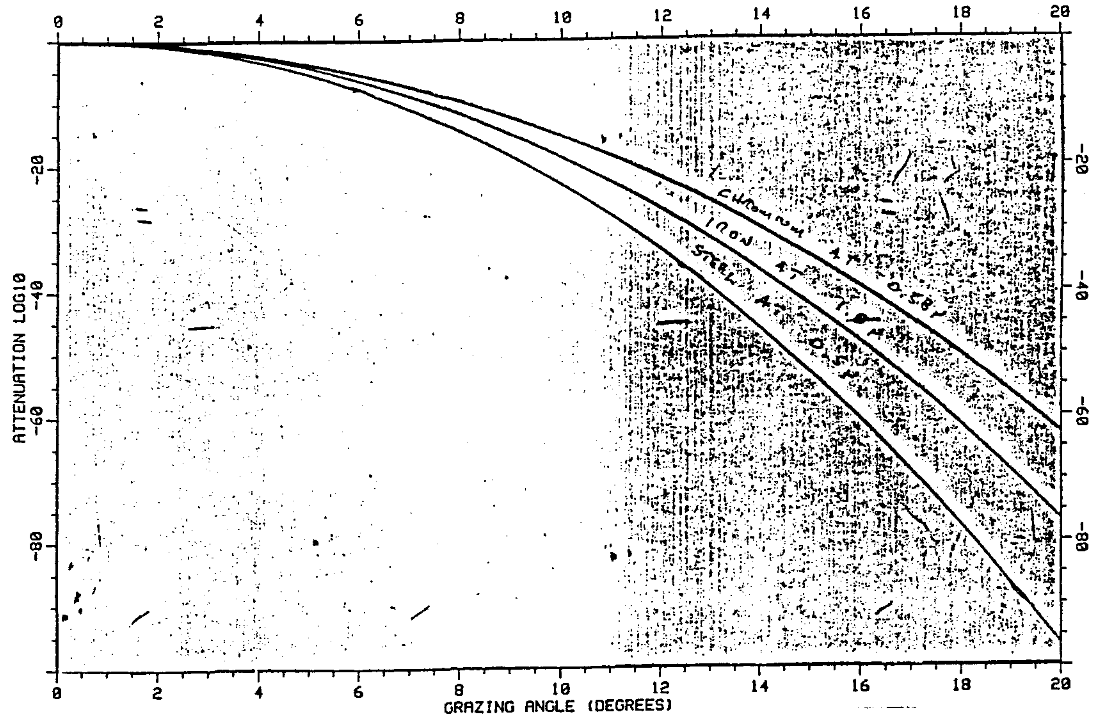

ATTENUATION 4Km LONG 48" DIAMETER TUBE

FIGURE 5

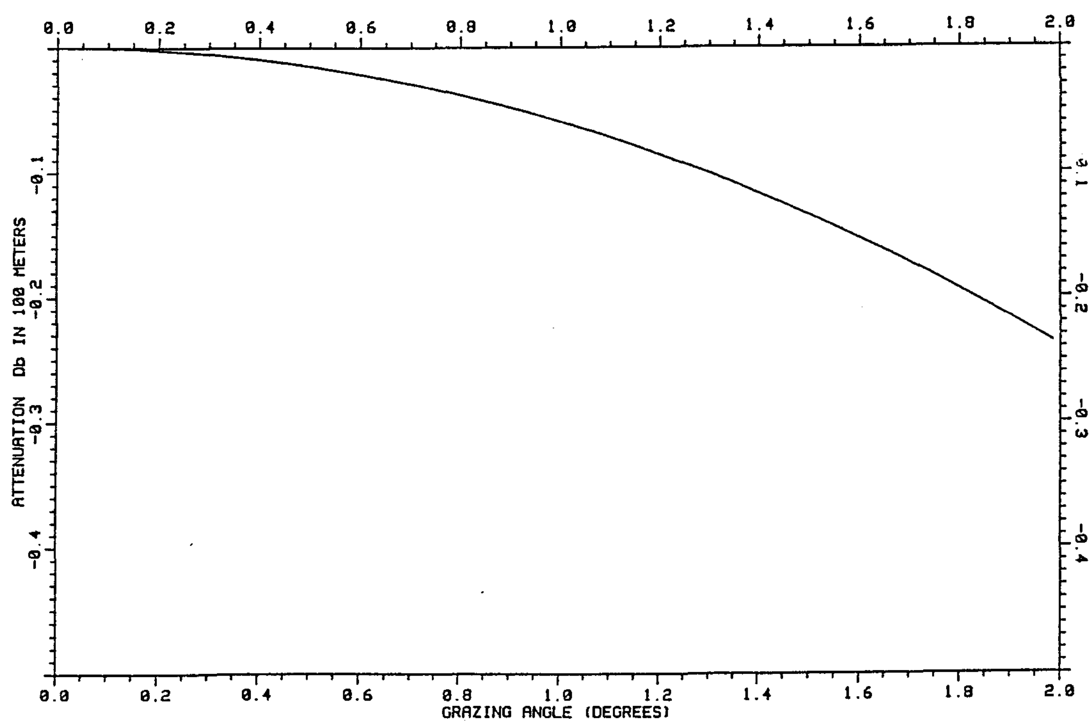

ATTENUATION DUE TO REFLECTION

STEEL

$R = R_{\perp}$

FIGURE 6

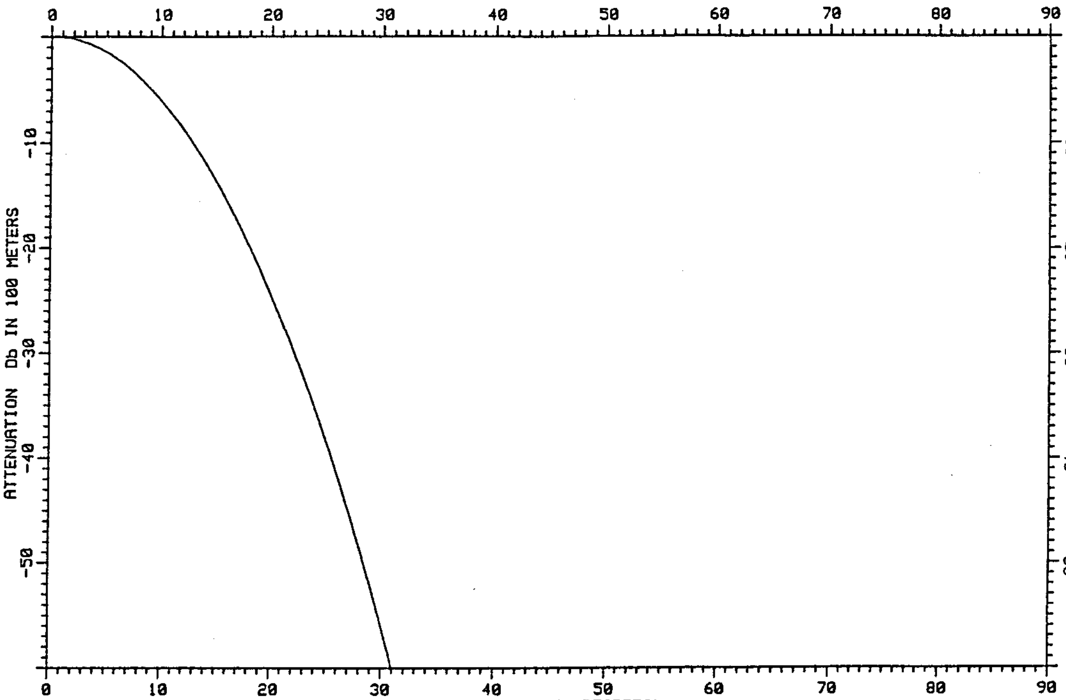

GRAZING ANGLE (DEGREES)

ATTENUATION DUE TO REFLECTION

6TEK L

Figure 7

$R = R_{\perp}$

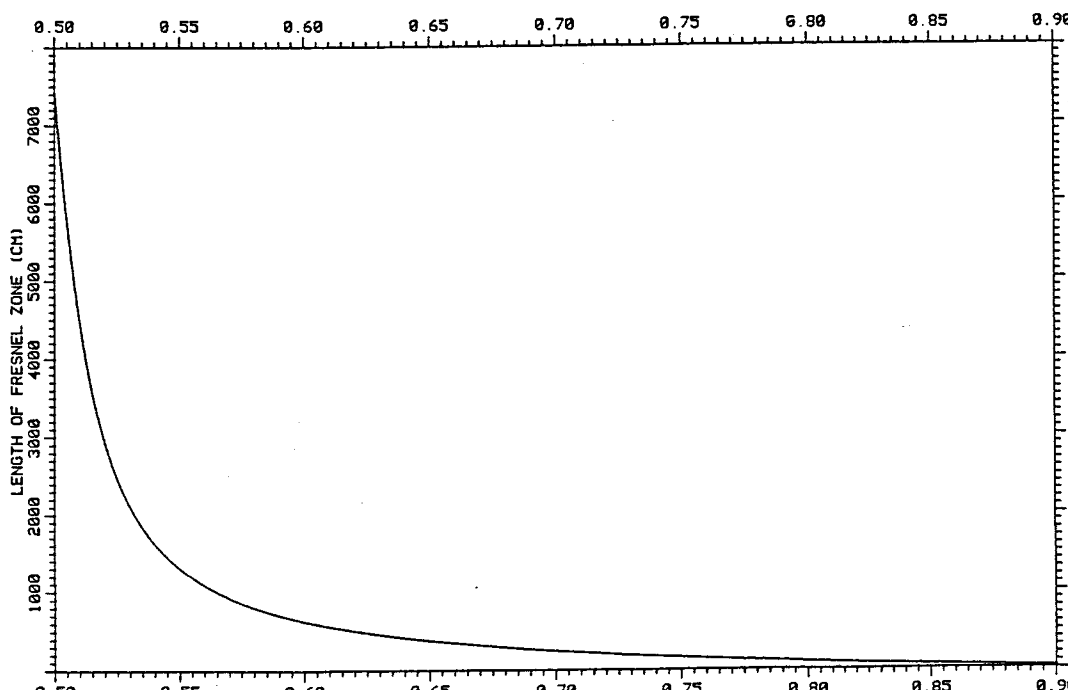

FRACTIONAL DISTANCE FROM END OF TUBE (4 KM TUBE)

SIZE OF FRESNEL ZONE ALONG 48 INCH DIMATER TUBE

Figure 8

$\lambda = 0.5\mu$

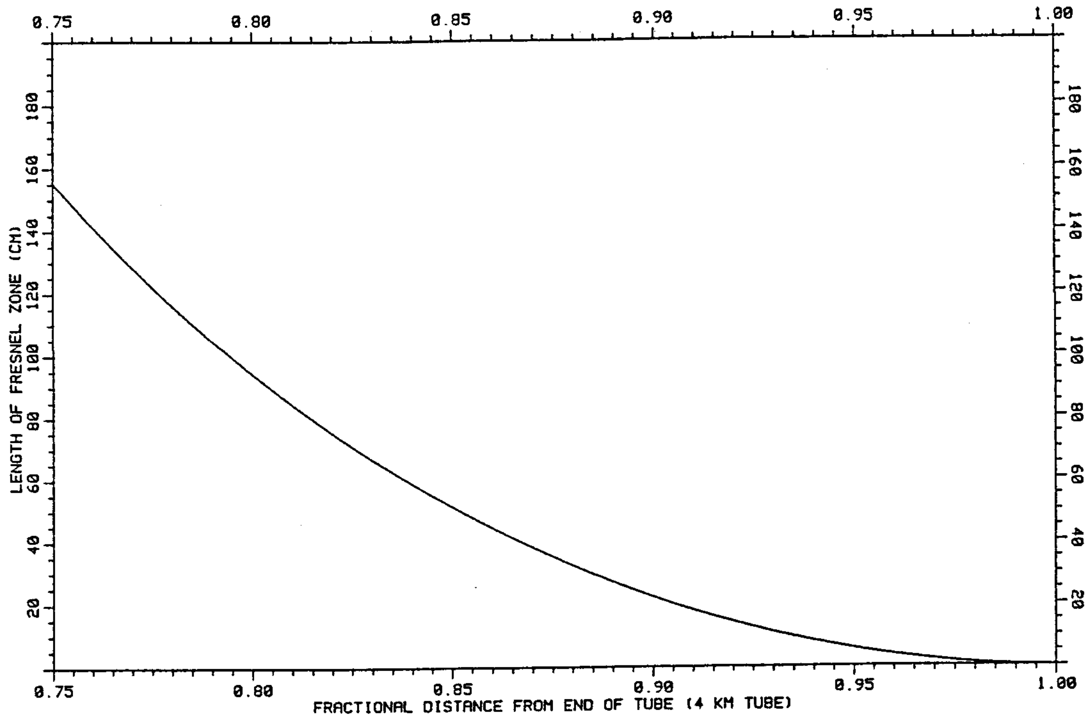

SIZE OF FRESNEL ZONE ALONG 48 INCH DIMATER TUBE

FIGURE 9

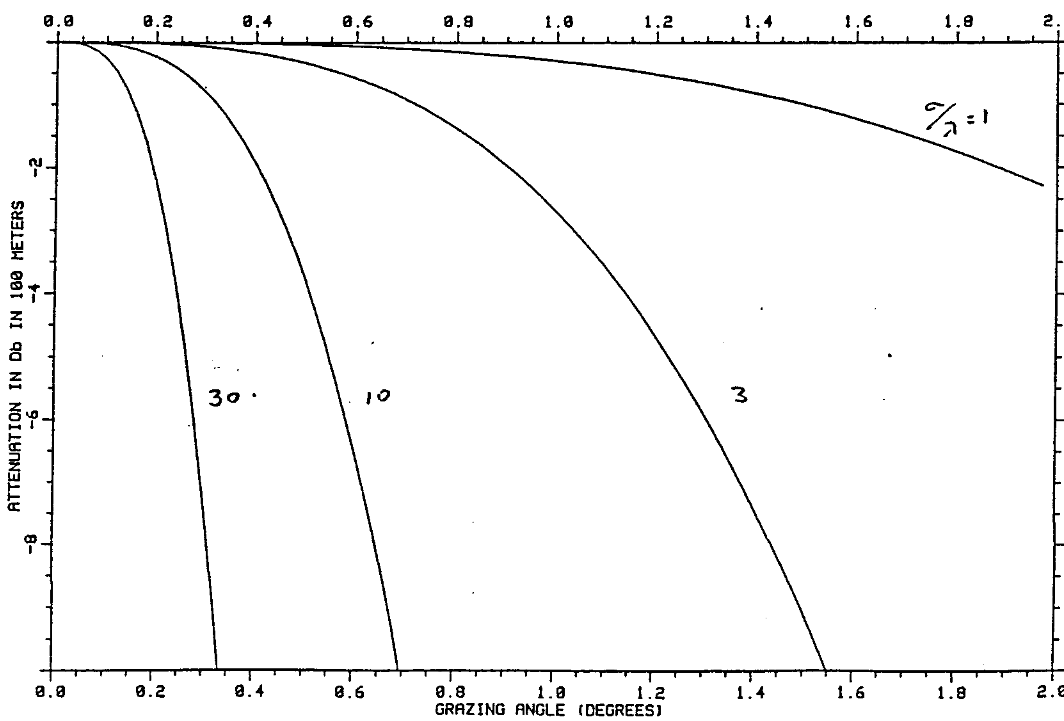

ATTENUATION OF SPECULAR (COHERENT) POWER

FIGURE 10

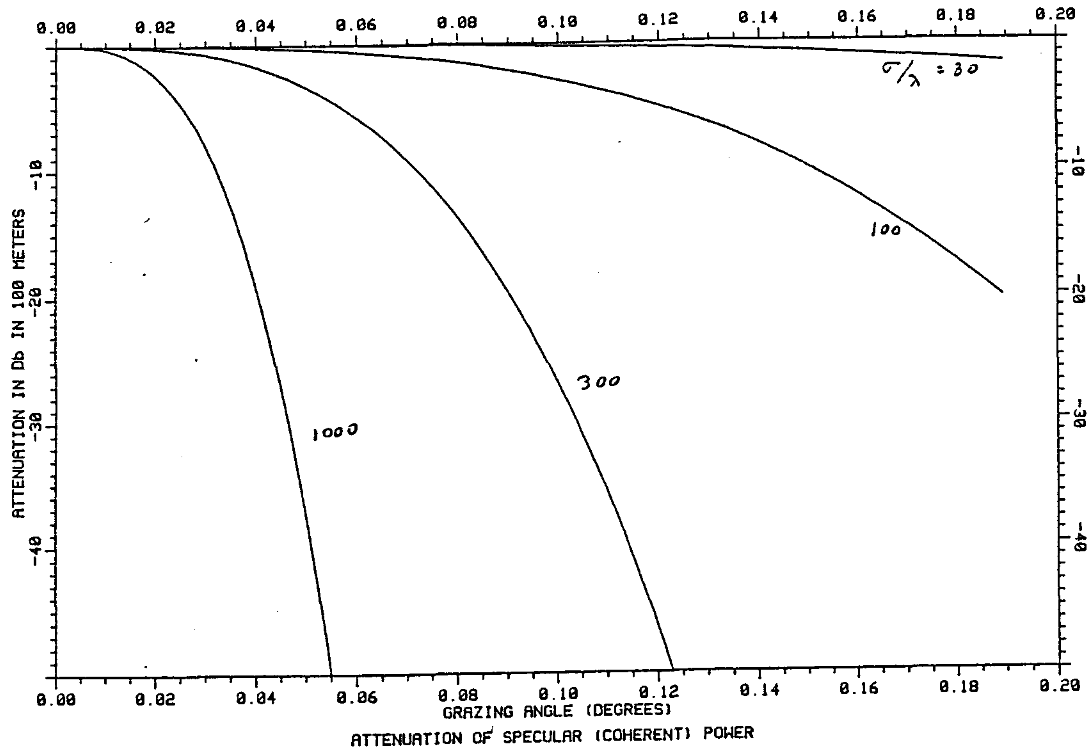

Figure 11

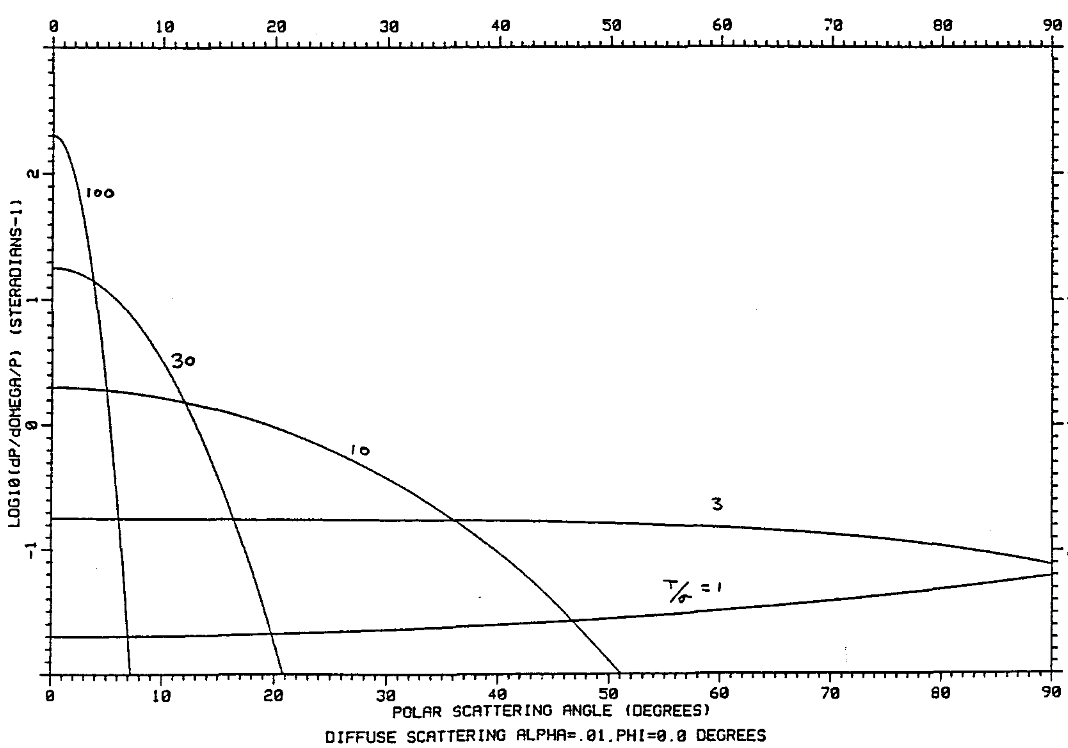

Figure 12

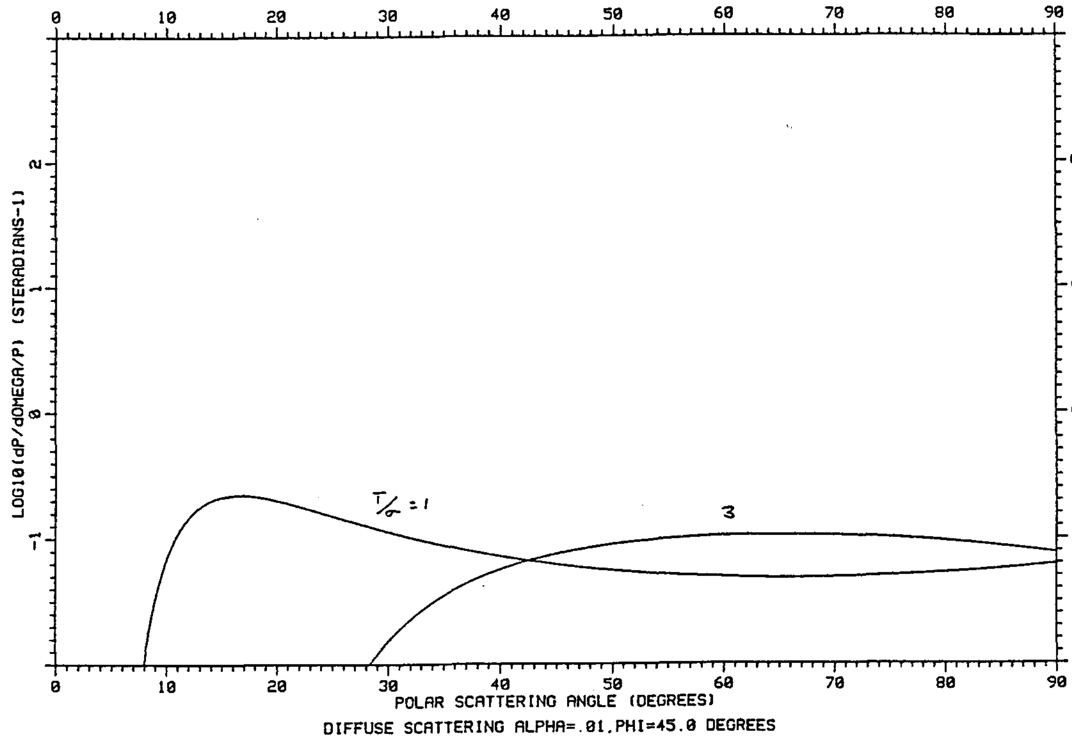

FIGURE 13

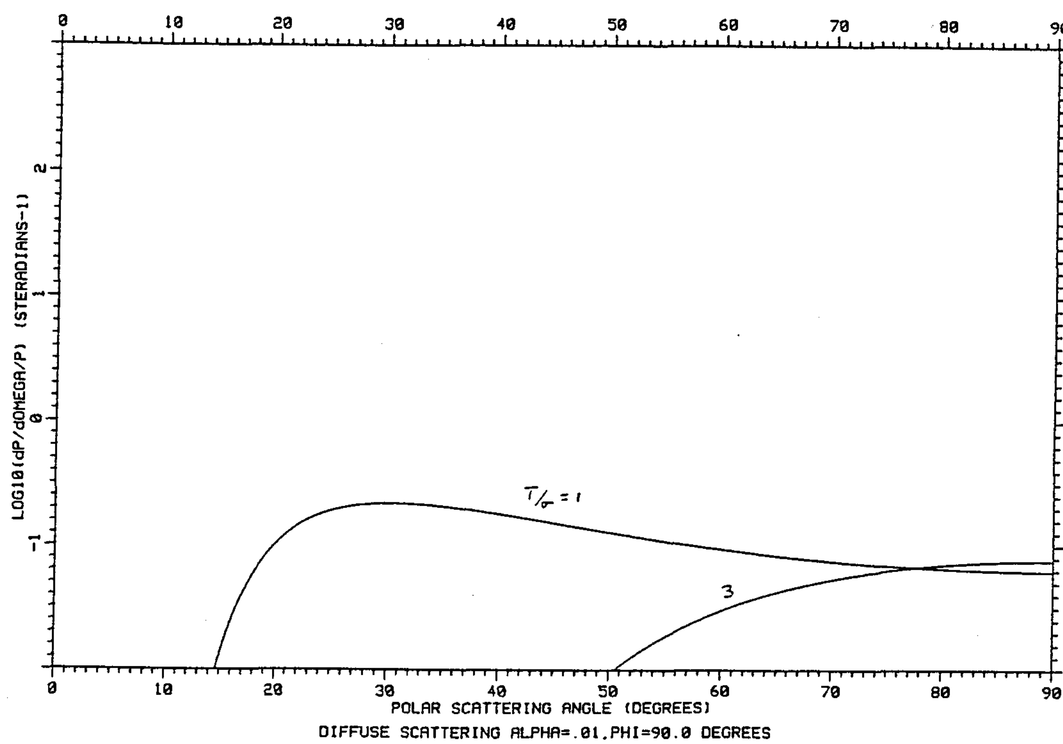

FIGURE 14

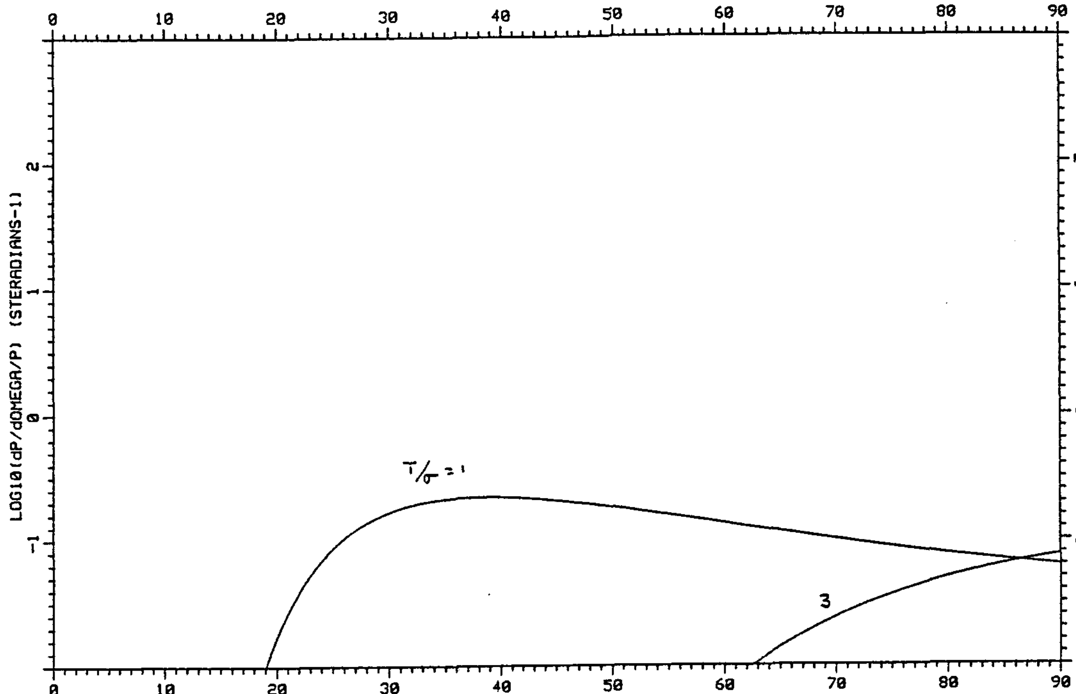

POLAR SCATTERING ANGLE (DEGREES)

DIFFUSE SCATTERING ALPHA=.01,PHI=135.0 DEGREES

FIGURE 15

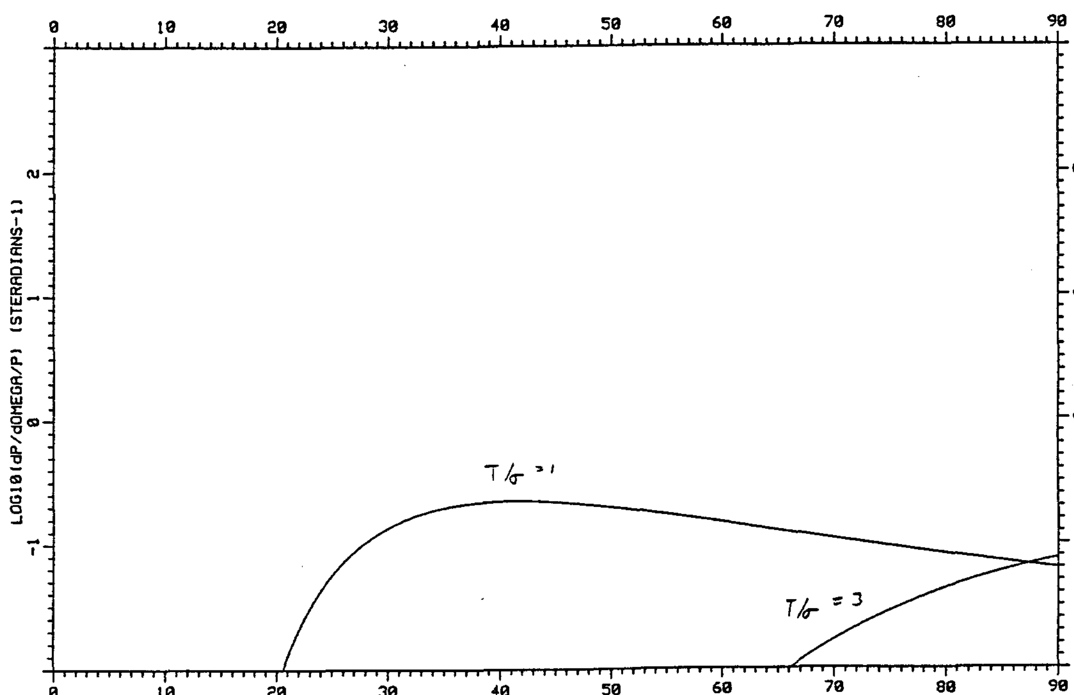

POLAR SCATTERING ANGLE (DEGREES)

DIFFUSE SCATTERING ALPHA=.01,PHI=180.0 DEGREES

FIGURE 16

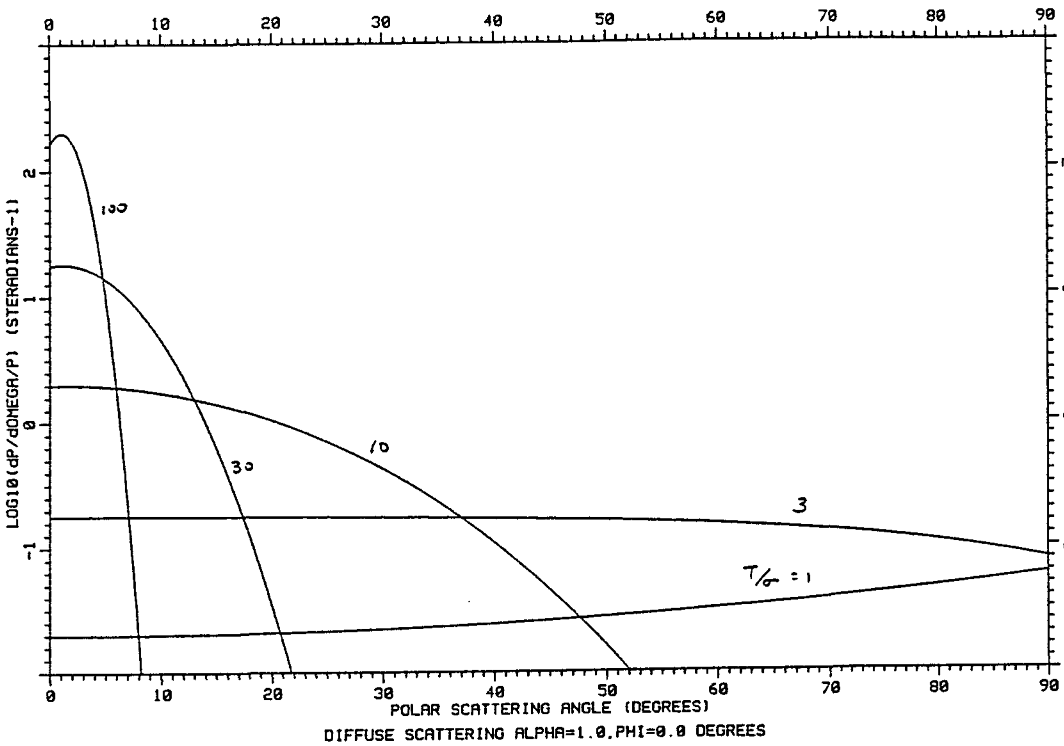

FIGURE 17

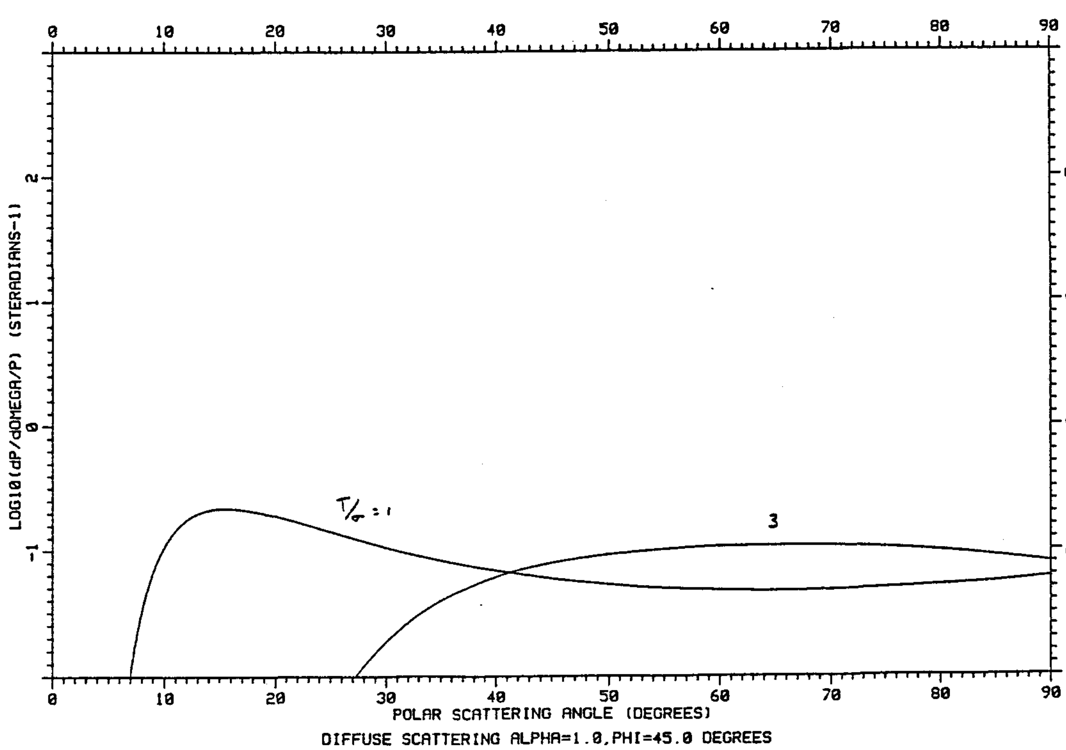

FIGURE 18

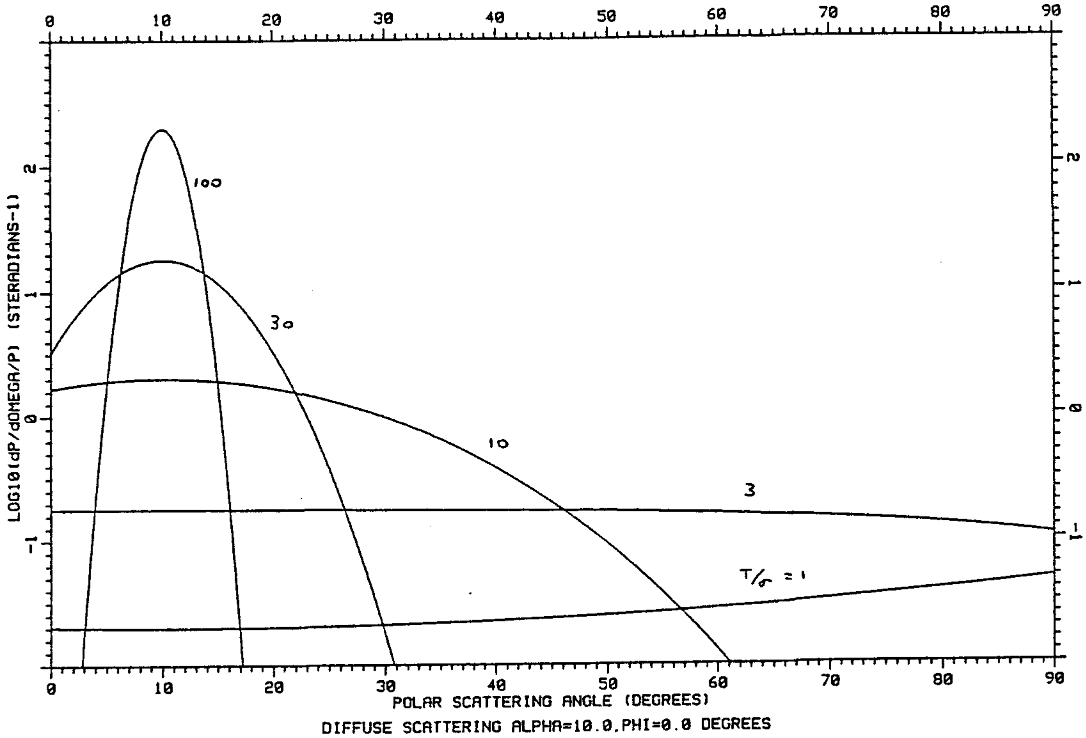

FIGURE 19

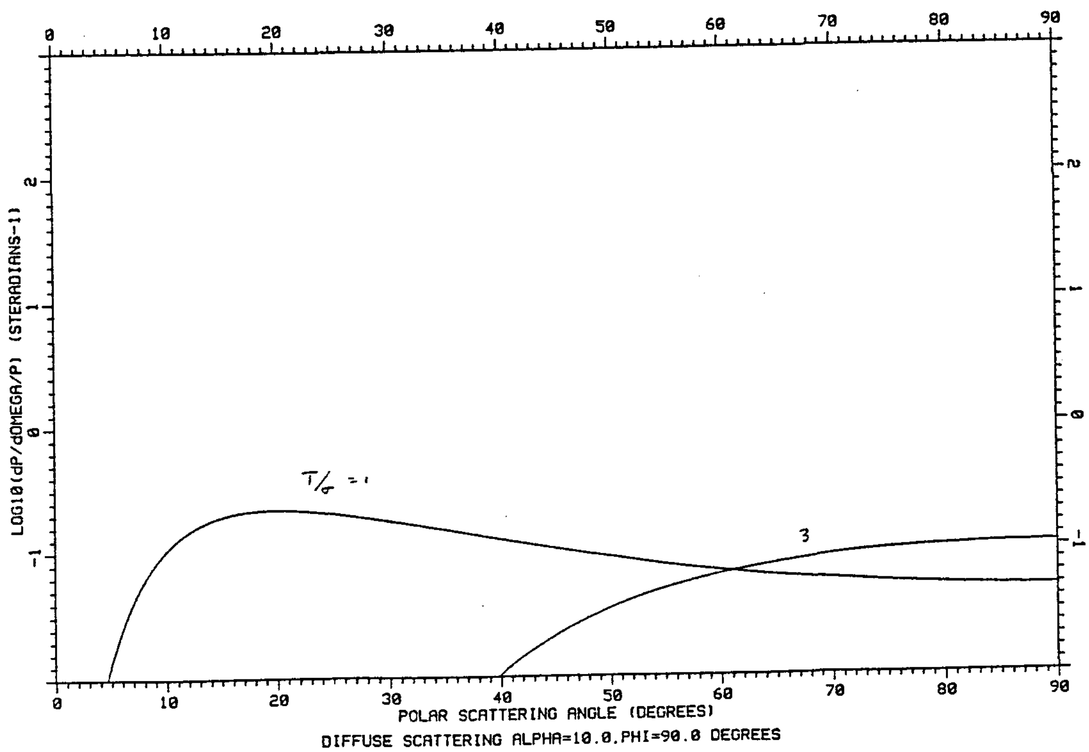

FIGURE 20

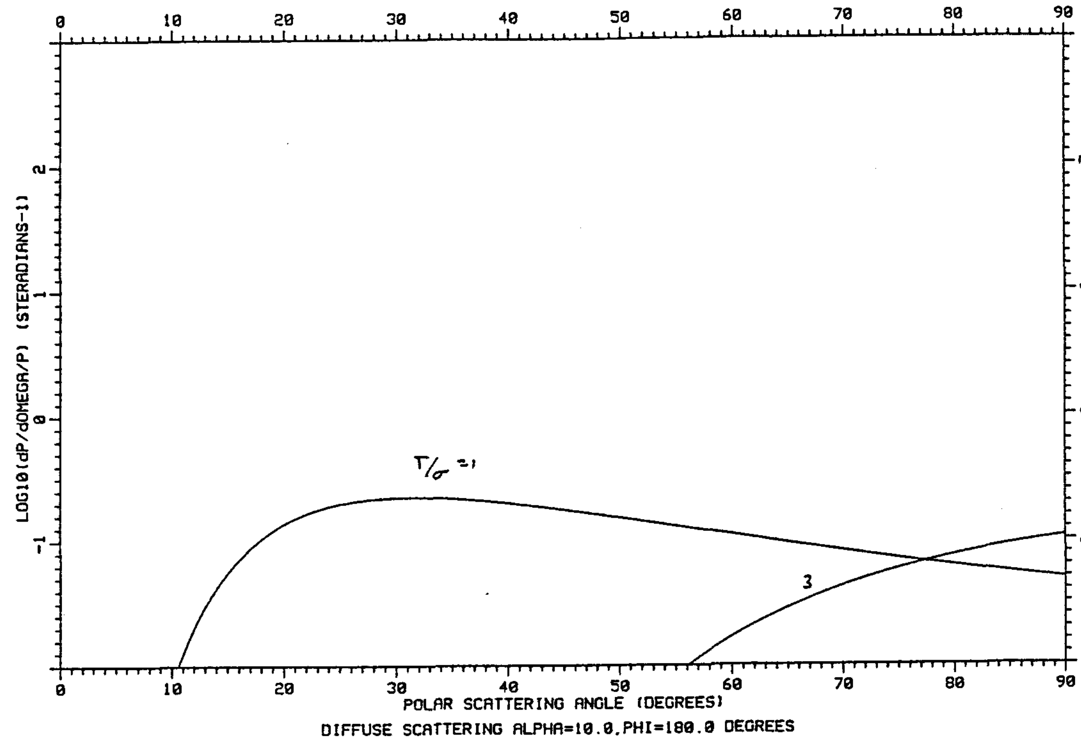

FIGURE 21

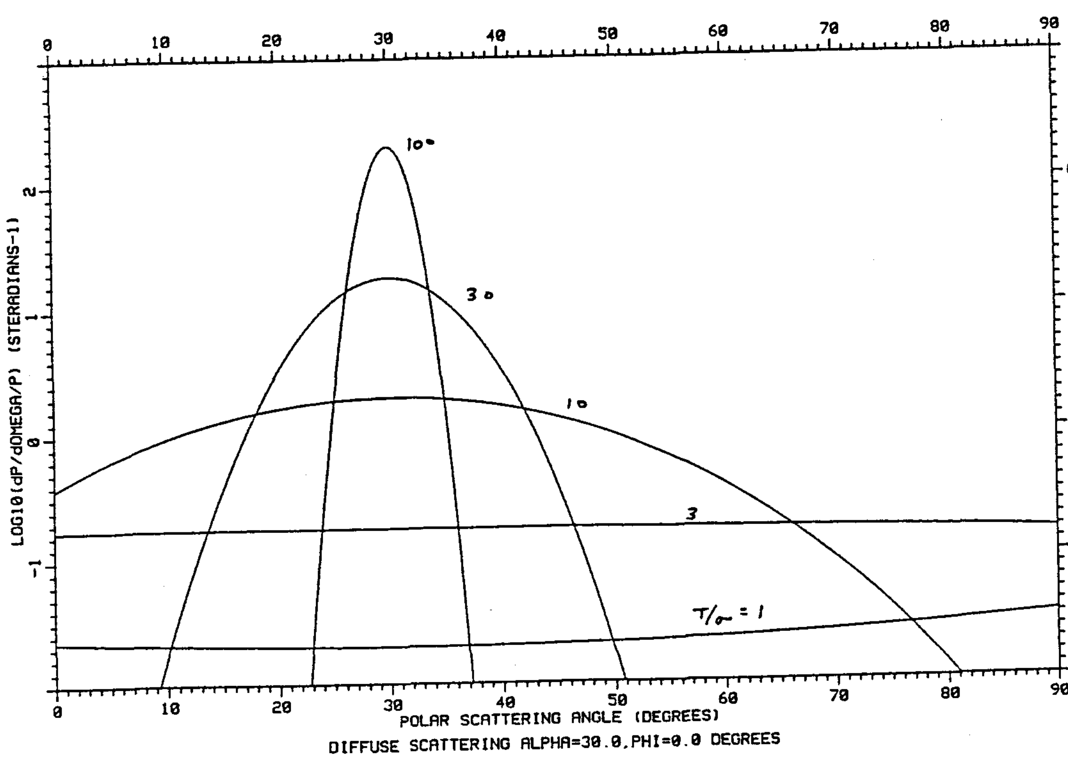

FIGURE 22

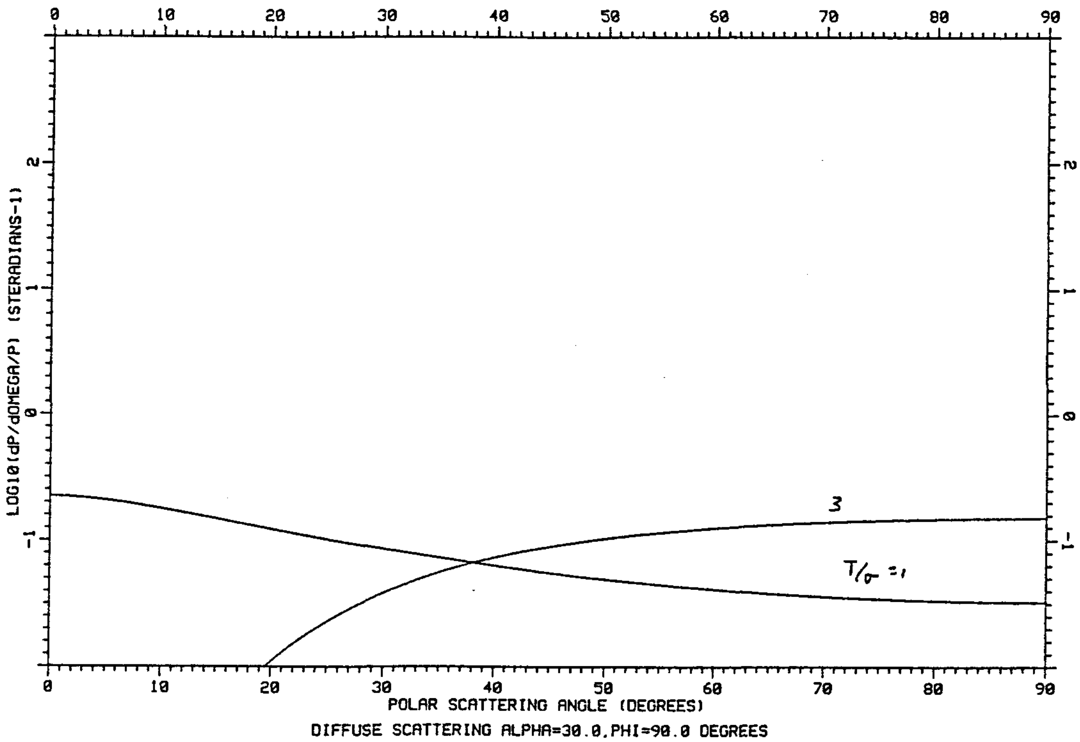

FIGURE 23

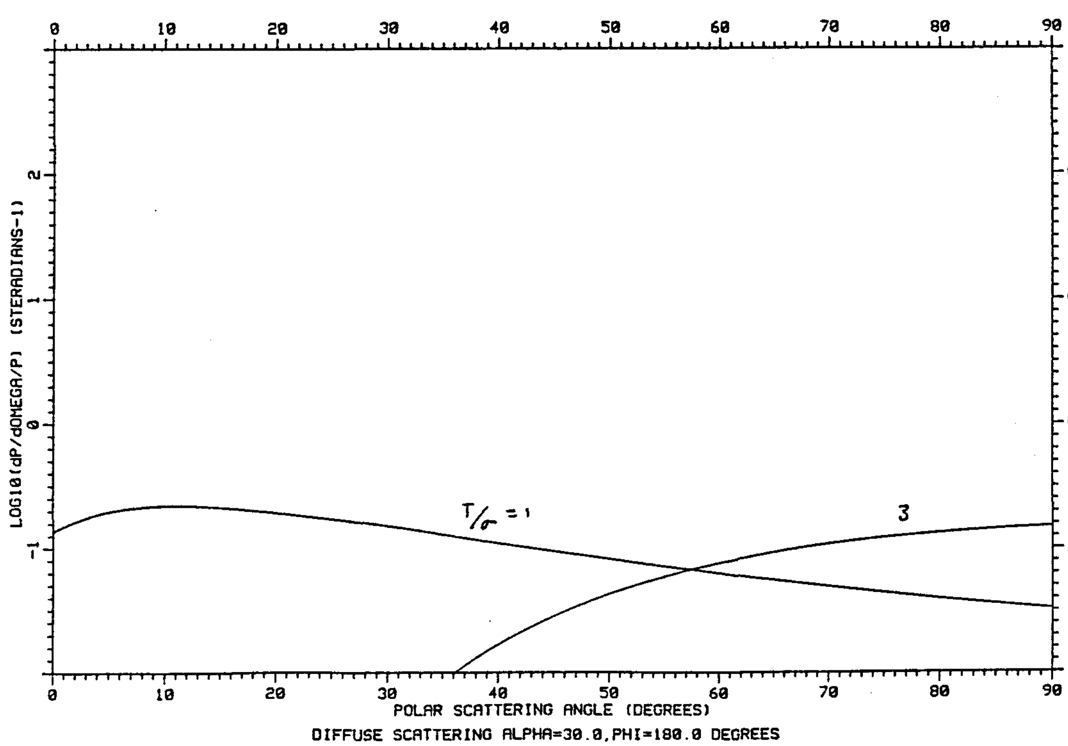

FIGURE 24

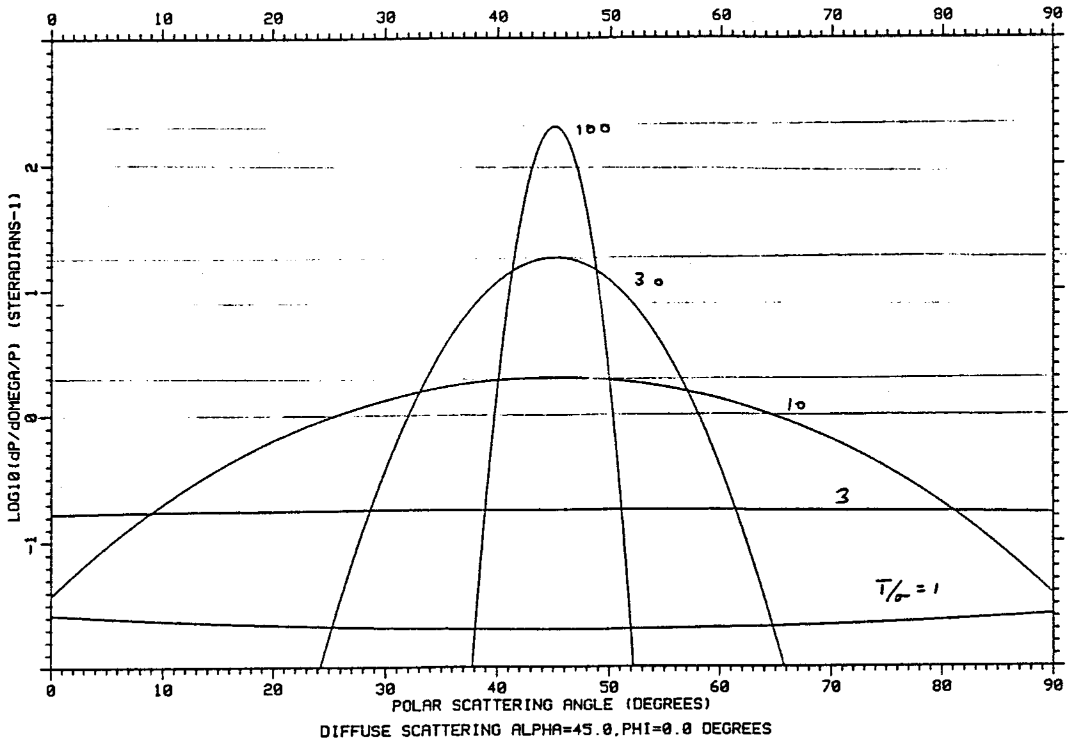

FIGURE 25

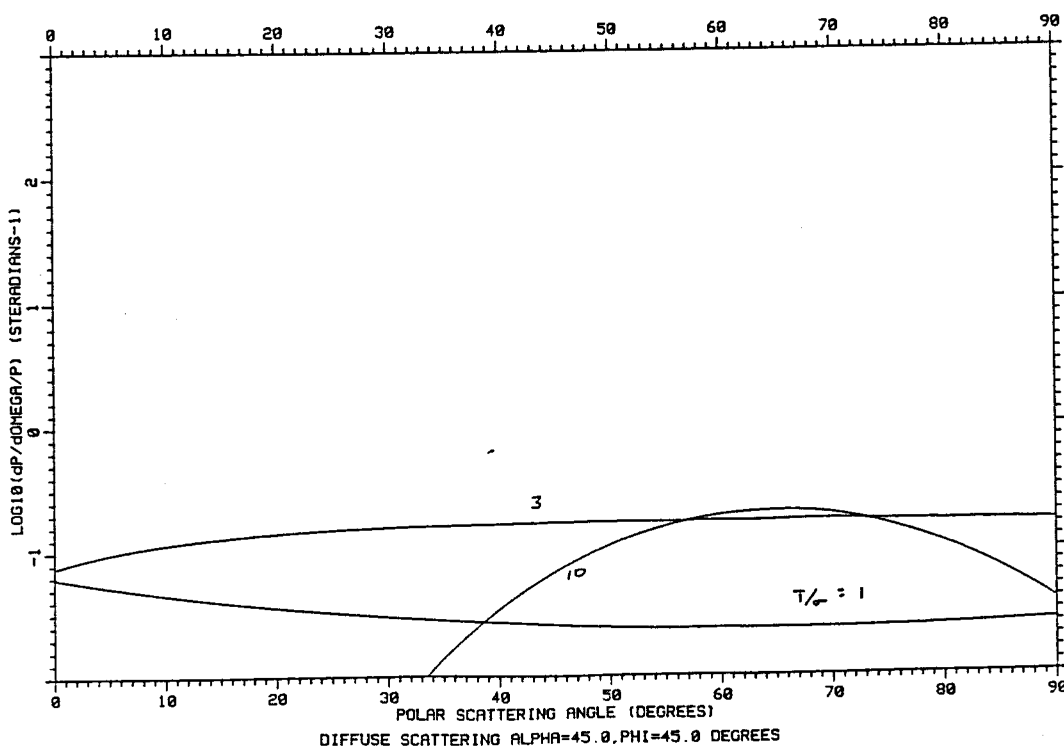

FIGURE 26

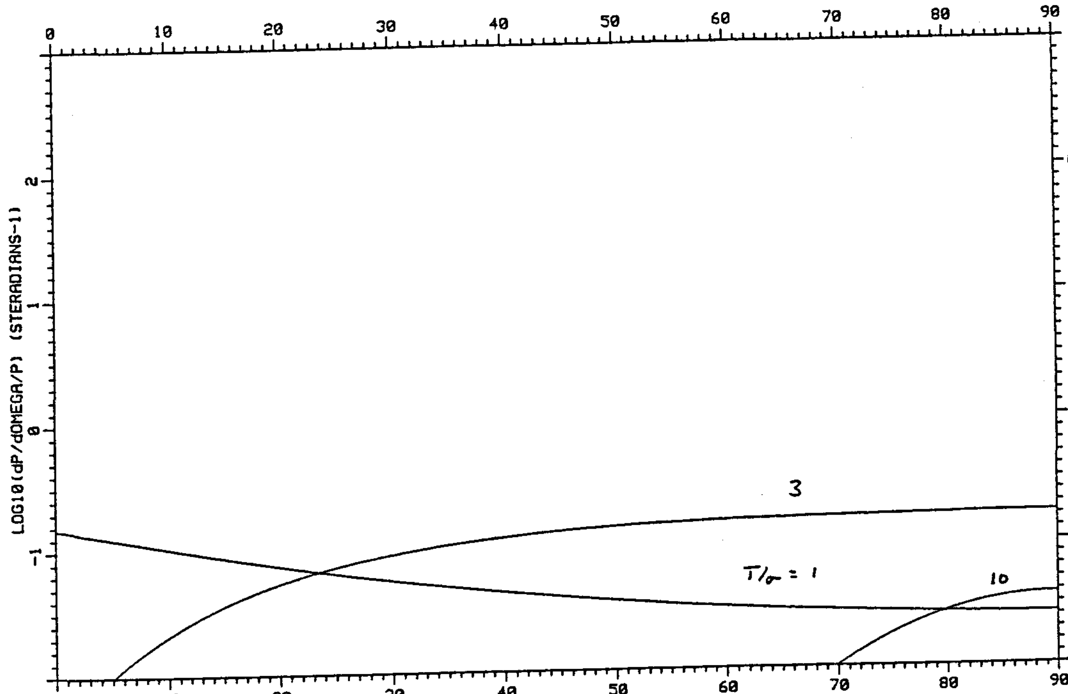

DIFFUSE SCATTERING ALPHA=45.0,PHI=90.0 DEGREES

FIGURE 27

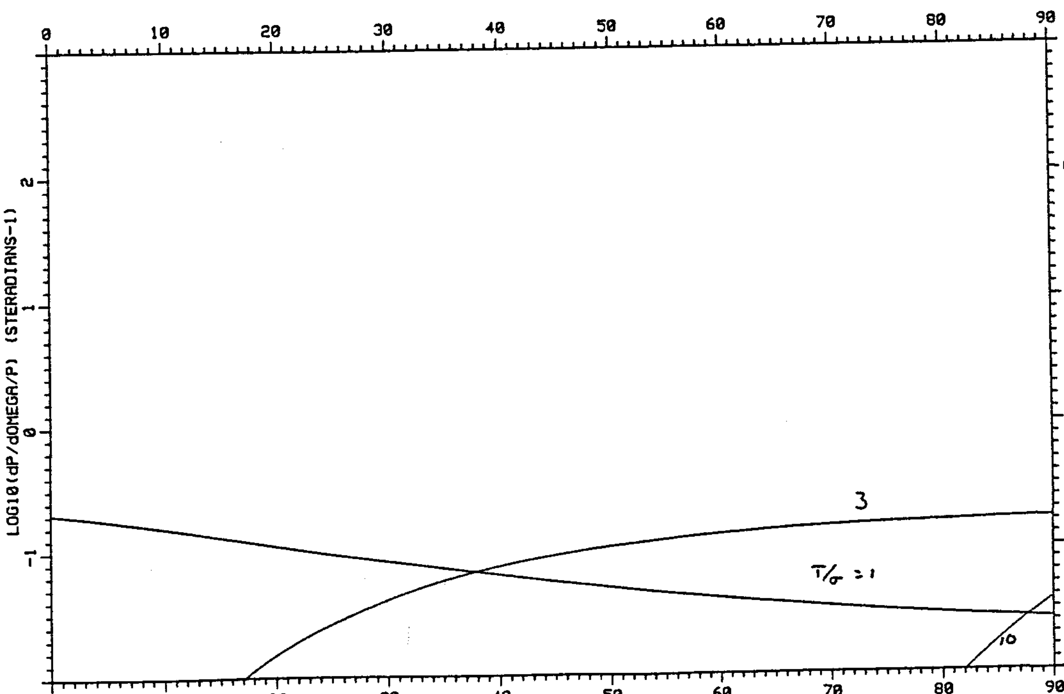

DIFFUSE SCATTERING ALPHA=45.0,PHI=135.0 DEGREES

FIGURE 28

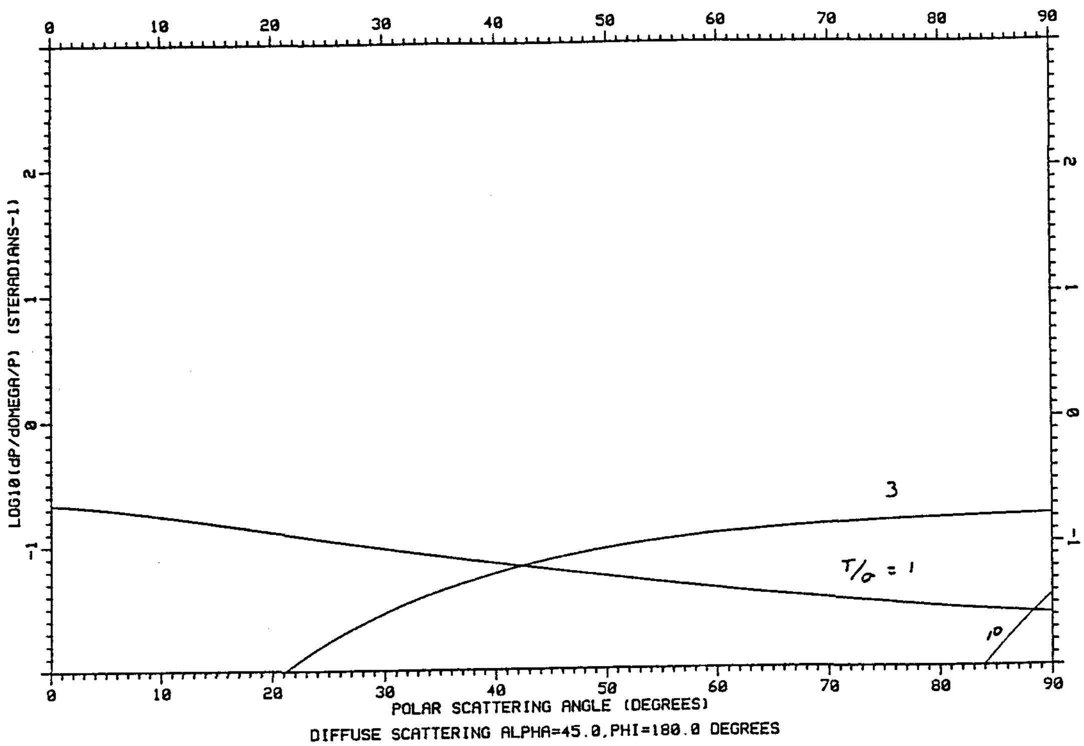

FIGURE 29

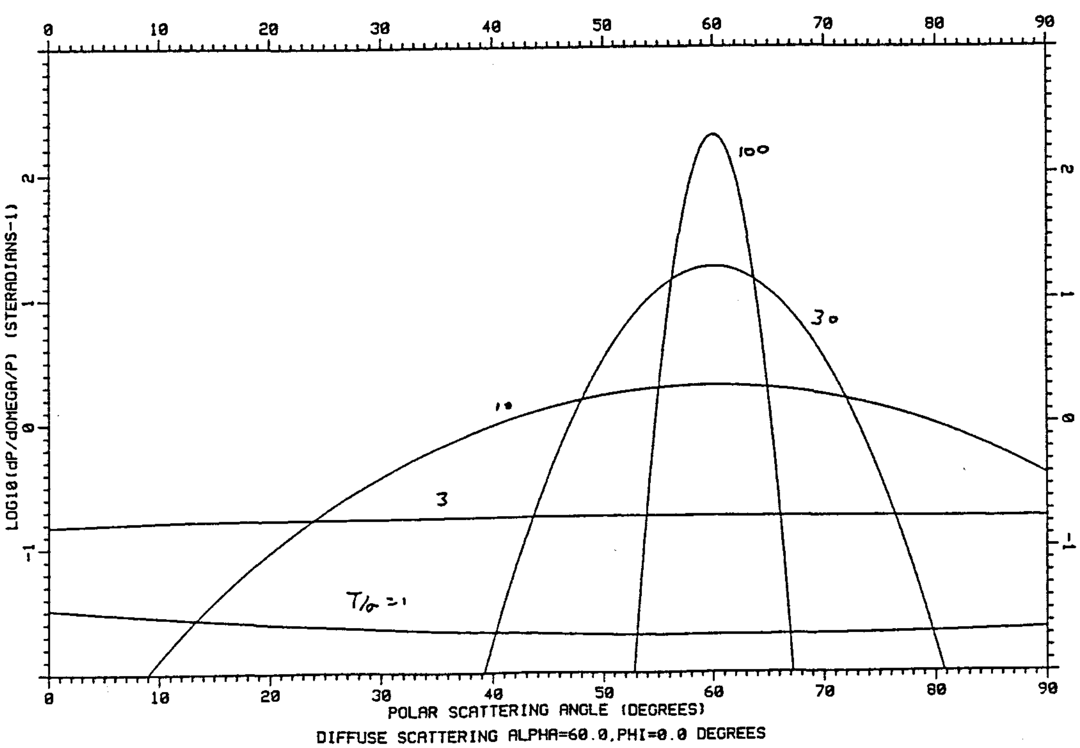

FIGURE 30